Monthly Notices
of the
ROYAL ASTRONOMICAL SOCIETY

Mon. Not. R. Astron. Soc. **407,** 1767–1772 (2010) doi:10.1111/j.1365-2966.2010.17008.x

Vertical stratification of iron in atmospheres of blue horizontal-branch stars

V. Khalack,[1⋆] F. LeBlanc[1] and B. B. Behr[2]

[1]*Département de Physique et d'Astronomie, Université de Moncton, Moncton, NB E1A 3E9, Canada*
[2]*Department of Systems Design Engineering, University of Waterloo, Waterloo, ON N2L 3G1, Canada*

Accepted 2010 May 11. Received 2010 May 10; in original form 2010 April 17

ABSTRACT

The aim of this study is to search for observational evidence of vertical iron stratification in the atmosphere of 14 blue horizontal-branch (BHB) stars. We have found from our numerical simulations that five BHB stars: B22, B186 in the globular cluster NGC 288, WF 2−820, WF 2−2692 in M13 and B203 in M15 show clear signatures of the vertical stratification of iron whose abundance increases toward the lower atmosphere. Two other BHB stars (B334 in M15 and B176 in M92) also show possible iron stratification in their atmosphere. A dependence of the slope of iron stratification on the effective temperature was also discovered. It is found that the vertical stratification of iron is strongest in BHB stars with $T_{\rm eff}$ around 11 500 K. The slope of iron abundance decreases as $T_{\rm eff}$ increases and becomes negligible for the BHB stars with $T_{\rm eff} \approx 14\,000$ K. These results support the hypothesis regarding the efficiency of atomic diffusion in the stellar atmospheres of BHB stars with $T_{\rm eff} \succeq 11\,500$ K.

Key words: stars: atmospheres – stars: chemically peculiar – stars: horizontal branch.

1 INTRODUCTION

According to the current understanding of stellar evolution, the horizontal-branch (HB) stars are post-main-sequence stars that burn helium in their core and hydrogen in a shell (e.g. Hoyle & Schwarzschild 1955; Moehler 2004). In this paper we consider the HB stars that are located in the blue part of the HB, to the left of the RR Lyrae instability strip. These stars are commonly called blue horizontal-branch (BHB) stars to distinguish them from the red horizontal-branch (RHB) stars, which exhibit different observational properties.

BHB stars with $T_{\rm eff} \succeq 11\,500$ K show several observational anomalies. By studying the position of BHB stars of globular clusters[1] on Hertzspruing–Russell diagrams, it is found that they exhibit photometric jumps (Grundhal et al. 1999) and gaps (Ferraro et al. 1998) at $T_{\rm eff} \simeq 11\,500$ K. These stars also show large abundance anomalies (Glaspey et al. 1989; Behr et al. 1999; Moehler et al. 1999; Behr 2003a). For instance, iron is generally overabundant in these stars relative to their cluster abundance. It is also found that the spectroscopic gravities of these stars are lower than those predicted by the canonical models (Crocker, Rood & O'Connell 1988; Moehler, Heber & DeBoer 1995). It is commonly believed that atomic diffusion of the elements in the atmosphere of these stars is responsible for the aforementioned observational anomalies. Atomic diffusion arises from the competition between radiative acceleration and gravitational settling. This can produce a net acceleration on atoms and ions, which results in their diffusion (Michaud 1970) and which may lead to abundance anomalies.

In addition to the detection of vertically stratified abundances in some BHB stars (Khalack et al. 2007, 2008, more information is given below), BHB stars with $T_{\rm eff} \succeq 11\,500$ K have lower rotational velocities than their cooler counterparts (Peterson, Rood & Crocker 1995; Behr, Cohen & McCarthy 2000b; Behr et al. 2000a; Behr 2003b). These observations suggest that the atmospheres of such stars are stable enough to have atomic diffusion. Theoretical results of Quievy et al. (2009) show that helium sinks in stars with low rotational velocities, which leads to the disappearance of the superficial He convection zone. This then opens the door for atomic diffusion to play a role.

Other theoretical results also concur with the belief that diffusion is present in the atmospheres of BHB stars with $T_{\rm eff} \succeq 11\,500$ K. For instance, the atmospheric models of Hui-Bon-Hoa, LeBlanc & Hauschildt (2000) showed that the observed photometric jumps and gaps for hot BHB stars can be explained by elemental diffusion in their atmosphere. These models calculate self-consistently the structure of the atmosphere while taking into account the stratification predicted by diffusion (assuming equilibrium). These models have recently been improved (LeBlanc et al. 2009) and confirm that vertical stratification of the elements can strongly modify the structure of the atmospheres of BHB stars. Such structural changes for the atmosphere lead to the photometric anomalies discussed above.

As mentioned above, by synthesizing spectral line profiles, Khalack et al. (2007) found vertical abundance stratification of sulfur in the atmosphere of the field BHB star HD 135485. Vertical

⋆E-mail: khalakv@umoncton.ca
[1] Most of the known BHB stars are found in globular clusters.

stratification of iron abundance was also detected by Khalack et al. (2008) in the atmosphere of two BHB stars in the globular cluster M15 and for one star in the globular cluster M13. Furthermore, more recently, Hubrig et al. (2009) have found isotopic anomalies of calcium in six BHB stars.

In this paper we will attempt to detect signatures of vertical abundance stratification of iron in a set of 14 BHB stars from line profile analysis for which we have appropriate data. This extension of the studies of Khalack et al. (2007, 2008) will serve to provide a larger amount of observational data for iron stratification which can then be used to verify theoretical models. We have selected the BHB stars from the spectra of Behr (2003a) relying on their value of effective temperature and their low $V \sin i$ ($\leq$10 km s^{-1}) so that atomic diffusion phenomena would most probably be present and detectable in these stars. The properties of the acquired spectra are discussed in Section 2, while in Section 3 the details concerning the simulation routine and adopted atmospheric parameters for the program stars are described. The evidence for vertical stratification of iron is given in Section 4 along with the estimation of the mean iron abundance, $V \sin i$ and radial velocities for each BHB star considered here. A discussion follows in Section 5.

2 OBSERVATIONS

The selected BHB stars were observed with the Keck I telescope and the High Resolution Echelle Spectrograph (HIRES). The stars were selected from the large sample of stars observed by Behr (2003a). The criteria by which the stars considered here were chosen is that their $T_{\rm eff}$ is close to or larger than 11 500 K and that they possess a low $V \sin i$ ($\leq$10 km s^{-1}). These criteria were chosen to maximize the chance that atomic diffusion is present in their atmosphere and that its effects are potentially observable.

Table 1 summarizes the information concerning the observations of the 14 stars chosen by giving (in individual columns) the object identification, the heliocentric Julian Date of the observation, the exposure time, the signal-to-noise ratio (S/N) per pixel, the spectral coverage, the effective temperature, the logarithm gravity and the heliocentric radial velocity.

The size of the C1 slit is 0.86 arcsec which provides a spectral resolution of $R = \lambda/\delta\lambda = 45\,000$. Behr (2003a) has found that for the aforementioned stars the underfilling of the slit should not change the estimated spectral resolution by more than 4–7 per cent. To process the spectra, Behr (2003a) has employed the package of routines developed by McCarthy (1990) for the FIGARO data analysis package (Shortridge 1993). A comprehensive description of the data acquisition and reduction procedure is presented by Behr (2003a).

3 SIMULATION PROCEDURE

The line profile simulations were performed with the ZEEMAN2 spectrum synthesis code (Landstreet 1988; Wade et al. 2001). Khalack & Wade (2006) have modified the ZEEMAN2 code to allow for an automatic minimization of the model parameters using the *downhill simplex method* (Press et al. 1992). To analyse the vertical abundance stratification we have built the dependence of the abundance derived from each analysed profile relative to the optical depth τ_{5000} for the list of selected line profiles, assuming that the profile is formed mainly at line optical depth $\tau_\ell = 1$. This depth corresponds to a continuum optical depth τ_{5000} of a certain value that in turn corresponds to a given layer of the stellar atmosphere model. A comprehensive description of the procedure is given by Khalack et al. (2007). This method was also used by Khalack et al. (2008) for the study of stratification in BHB stars and by Thiam et al. (2010) for HgMn stars.

The stellar atmosphere models used for our analysis were calculated with the PHOENIX code (Hauschildt, Baron & Allard 1997) assuming local thermodynamic equilibrium (LTE), solar metallicity except for the iron abundance and depleted helium abundances and the surface gravities extracted from Behr (2003a) which are listed in Table 1. The depleted helium abundance has also been taken into account during line profile simulations using ZEEMAN2.

In a previous study, Khalack et al. (2008) showed that inclusion of non-zero microturbulence leads to the amplification of signatures of vertical abundance stratification for different chemical species. Therefore, in order to mitigate the influence of microturbulence on the estimation of iron vertical stratification, we have assumed zero microturbulent velocity in the simulations presented here.

Table 1. Journal of Keck+HIRES spectroscopic observations of the selected hot BHB stars from Behr (2003a).

Cluster/star	HJD (245 0000+)	Exposure time (s)	S/N	Coverage (Å)	$T_{\rm eff}$ (K)	log g (dex)	$V \sin i$ (km s^{-1})	$V_{\rm r}$ (km s^{-1})	[Fe/H]	[He/H]
M13/WF 2−820	1052.7815	3 × 1200	34	3888–5356	11 840	3.90	4.17	-239.7 ± 0.7	$-0.22^{+0.14}_{-0.23}$	$-1.09^{+0.47}_{-0.44}$
M13/WF 2−2692	1047.7400	3 × 1800	34	3885–6292	12 530	4.08	4.64	-236.2 ± 0.7	$-0.23^{+0.76}_{-0.34}$	$-1.81^{+0.96}_{-1.07}$
M13/WF 2−3123	1248.1298	3 × 1200	35	3885–6292	13 670	4.31	6.32	-238.3 ± 1.1	$-0.71^{+0.65}_{-0.51}$	$-1.28^{+1.55}_{-0.92}$
M13/WF 3−548	1053.7293	3 × 1200	32	3888–5356	13 100	4.16	4.29	-235.3 ± 0.7	$-0.64^{+0.60}_{-0.35}$	$-2.10^{+1.08}_{-0.98}$
M13/WF 3−1718	1248.0811	3 × 1200	48	3888–5884	11 510	3.79	1.89	-244.0 ± 0.3	$+0.02^{+0.10}_{-0.13}$	$-1.86^{+0.42}_{-0.68}$
M15/B203	1408.0180	3 × 1200	28	3885–6292	13 990	3.84	4.89	-94.7 ± 1.2	$+0.02^{+0.38}_{-0.42}$	$-2.54^{+1.15}_{-0.67}$
M15/B315	1409.0238	3 × 1200	24	3885–6292	12 890	3.81	1.72	-103.3 ± 0.8	$+0.04^{+0.44}_{-0.36}$	$-1.75^{+0.94}_{-0.99}$
M15/B334	1052.8791	4 × 1500	39	3888–5356	10 750	3.61	9.22	-109.3 ± 1.3	$-2.37^{+0.19}_{-0.21}$	$-0.64^{+0.45}_{-0.45}$
M15/B374	1406.0183	3 × 1200	21	3885–6292	12 820	3.82	3.92	-106.5 ± 0.9	$+0.24^{+0.48}_{-0.37}$	$-1.97^{+0.94}_{-0.92}$
M92/B176	1049.0646	3 × 1800	56	4020–5520	11 150	3.76	6.96	-116.3 ± 1.4	$-2.25^{+0.16}_{-0.24}$	$-0.55^{+0.36}_{-0.32}$
NGC 288/B16	1406.0850	3 × 1200	21	3885–6292	14 030	4.15	3.08	-44.7 ± 0.9	$+0.66^{+0.65}_{-0.49}$	$-2.82^{+0.91}_{-0.71}$
NGC 288/B22	1407.0955	3 × 1200	17	3885–6292	12 130	4.01	2.48	-43.8 ± 0.9	$+0.28^{+0.29}_{-0.38}$	$-2.36^{+1.26}_{-0.64}$
NGC 288/B186	1409.0862	3 × 1200	31	3885–6292	11 390	3.94	3.89	-43.8 ± 0.5	$+0.17^{+0.17}_{-0.21}$	$-1.45^{+0.65}_{-0.85}$
NGC 288/B302	1408.0891	3 × 1200	26	3885–6292	13 230	4.15	1.85	-43.8 ± 0.5	$+0.61^{+0.34}_{-0.32}$	$-2.63^{+0.88}_{-0.66}$

Table 2. Properties of the BHB stars studied here.

Cluster/star	[Fe/H]	$V \sin i$ (km s^{-1})	V_r (km s^{-1})	n
M13/WF 2−820	-0.09 ± 0.32	4.2 ± 1.0	-239.6 ± 0.8	79
M13/WF 2−2692	$+0.03 \pm 0.25$	4.4 ± 1.0	-236.2 ± 1.0	74
M13/WF 2−3123	-0.57 ± 0.17	6.0 ± 1.5	-238.3 ± 1.0	21
M13/WF 3−548	-0.49 ± 0.16	4.2 ± 0.7	-235.0 ± 1.3	26
M13/WF 3−1718	$+0.14 \pm 0.13$	2.0 ± 0.3	-243.7 ± 0.7	96
M15/B203	-0.14 ± 0.22	5.1 ± 1.3	-95.0 ± 0.3	32
M15/B315	$+0.10 \pm 0.21$	1.8 ± 0.2	-103.2 ± 0.9	72
M15/B334	-1.38 ± 0.86	10.1 ± 0.5	-106.5 ± 2.1	11
M15/B374	$+0.59 \pm 0.21$	4.0 ± 0.9	-107.0 ± 1.1	82
M92/B176	-1.26 ± 0.75	7.0 ± 1.0	-117.7 ± 1.2	21
NGC 288/B16	$+0.69 \pm 0.15$	2.9 ± 0.9	-45.1 ± 0.9	42
NGC 288/B22	$+0.52 \pm 0.22$	2.5 ± 0.5	-43.9 ± 0.8	47
NGC 288/B186	$+0.40 \pm 0.17$	3.3 ± 0.8	-43.9 ± 0.5	65
NGC 288/B302	$+0.77 \pm 0.17$	1.8 ± 0.2	-44.0 ± 0.5	75

In this paper, we have selected a list of Fe II lines that are suitable for abundance and stratification analysis. The full list of the analysed spectral lines is given in the electronic version of the article (Table S1 – see Supporting Information). Atomic data for Fe II lines are extracted from VALD-2 (Raassen & Uylings 1998[2]; Kupka et al. 1999; Ryabchikova et al. 1999; Pickering, Thorne & Perez 2001) line data base.

4 IRON VERTICAL STRATIFICATION

A sample of 14 BHB stars from the globular clusters M13, M15, M92 and NGC 288 were studied using the procedure briefly described in Section 3. These stars were chosen using the criteria described in Section 2 and some of their properties obtained by our analysis are listed in Table 2, namely, their average iron abundance, $V \sin i$ and mean heliocentric radial velocity averaged over all lines analysed (n represents the number of lines). The reported uncertainties are equal to the standard deviation calculated from the results of individual line simulations for all lines considered. The results shown in Table 2 for the iron abundance are consistent to those found by Behr (2003a) (see Table 1) except for the stars B334 and B176. This difference is partly due to the fact that Behr (2003a) used mainly strong iron lines for his analysis while we also use weak lines which are formed deeper in the atmosphere and predict larger average iron abundance. A larger abundance is obtained because these two stars show an enhancement of iron abundance in the deeper atmospheric layers. The radial velocities found here are also consistent for all the stars, but once again the stars B334 and B176 show a small difference between our results and those of Behr (2003a). These two stars will be discussed in more detail below.

The effective temperatures of the BHB stars studied here range from 10 750 to 14 030 K (see Table 1). This and the variety of the mean abundance values for iron (see Table 2) among the sample of BHB stars provide a unique opportunity to search for evidence of abundance vertical stratification of iron and to estimate its possible relation to other physical characteristics of these stars.

[2] http://www.science.uva.nl/pub/orth/

4.1 Search for signatures of vertical stratification

To verify if iron abundance is vertically stratified in the stellar atmospheres of the selected BHB stars, we have analysed individually all Fe II line profiles present in the spectra that give small errors for the estimated parameters (iron abundance, V_r and $V \sin i$), assuming zero microturbulence. The measured abundance for each line was then associated to a line depth formation. The iron abundances obtained for different optical depths (see Fig. 1) were fitted to a linear function (for the range of atmospheric depths $-5.3 < \log \tau_{5000} < -2.0$) using the least-square algorithm to statistically evaluate the significance of observable trends. This range of $\log \tau_{5000}$ was chosen because spectra from our sample of stars all possess iron lines within this interval. The main result found here is that the iron abundance generally increases towards the deeper atmosphere, although some of the increases found are not statistically significant. The slope of these gradients is presented in Table 3, where the individual columns give the increase of $\log N_{Fe}/N_{tot}$ (in dex) calculated per dex of $\log \tau_{5000}$, the average iron abundance value obtained taking into account all of the lines and the number of lines analysed. Without further analysis, it is found that among our sample of 14 stars, seven stars show clear signatures of vertical stratification of iron. Two of them (B22 and B186) are located in the globular cluster NGC 288, two (WF 2−820 and WF 2−2692) in M13, two (B203 and B334) in M15 and one (B176) in M92 (see Fig. 1 and Table 3). One more BHB star, B302 (in NGC 288) also shows a slope that is statistically significant (with respect to the error bar), but its value is too low to confidently state, due to all of the uncertainties inherent to line analysis, that iron stratification exists in this star.

However, for two of the seven BHB stars that show iron stratification (B334 and B176), iron is strongly depleted (in comparison with the solar abundance of iron) and the number of analysed iron lines is therefore respectively smaller than for most of the other stars studied here (see Table 3). However, the iron abundance at $\log \tau_{5000} = -2$ is nearly solar and is therefore higher than the cluster abundance. The same two stars show very large slopes for the iron abundance with respect to optical depth (see bottom row of Fig. 1). Since our analysis is based on a relatively small number of lines (especially for B334), these results could be distorted by few cases of line misidentification. It is also surprising that such a large stratification slope is found where iron abundance is not enhanced in the outer atmosphere and helium abundance is large. If diffusion were at play, a larger iron abundance and a smaller helium abundance would be expected. These two stars also appear to have radial velocities, determined from the analysis of Fe II lines, slightly different (even though this difference is inside the error bars it is greater than for the other stars of our sample) than those obtained by Behr (2003a) from the combined analysis of lines of different chemical species. The average iron abundance found here for these two stars (see Table 2) are quite different form those found by Behr (2003a) (see Table 1), but this is due to the fact that we have also studied some weaker lines (see Section 4.1). Therefore, all of these discrepancies cast some doubts about our results for these two stars and therefore more high-quality spectra is needed to confirm the presence of iron stratification in their atmosphere.

The vertical iron stratification for the other five stars: WF 2−820 and WF 2−2692 in M13, B22 and B186 in NGC 288 and B203 in M13 is shown in Fig. 1. The lines used to produce these figures span several orders of magnitude for τ_{5000}. Furthermore, since the increase of the abundance along this depth range is too large to be explained by the various uncertainties intervening in abundance

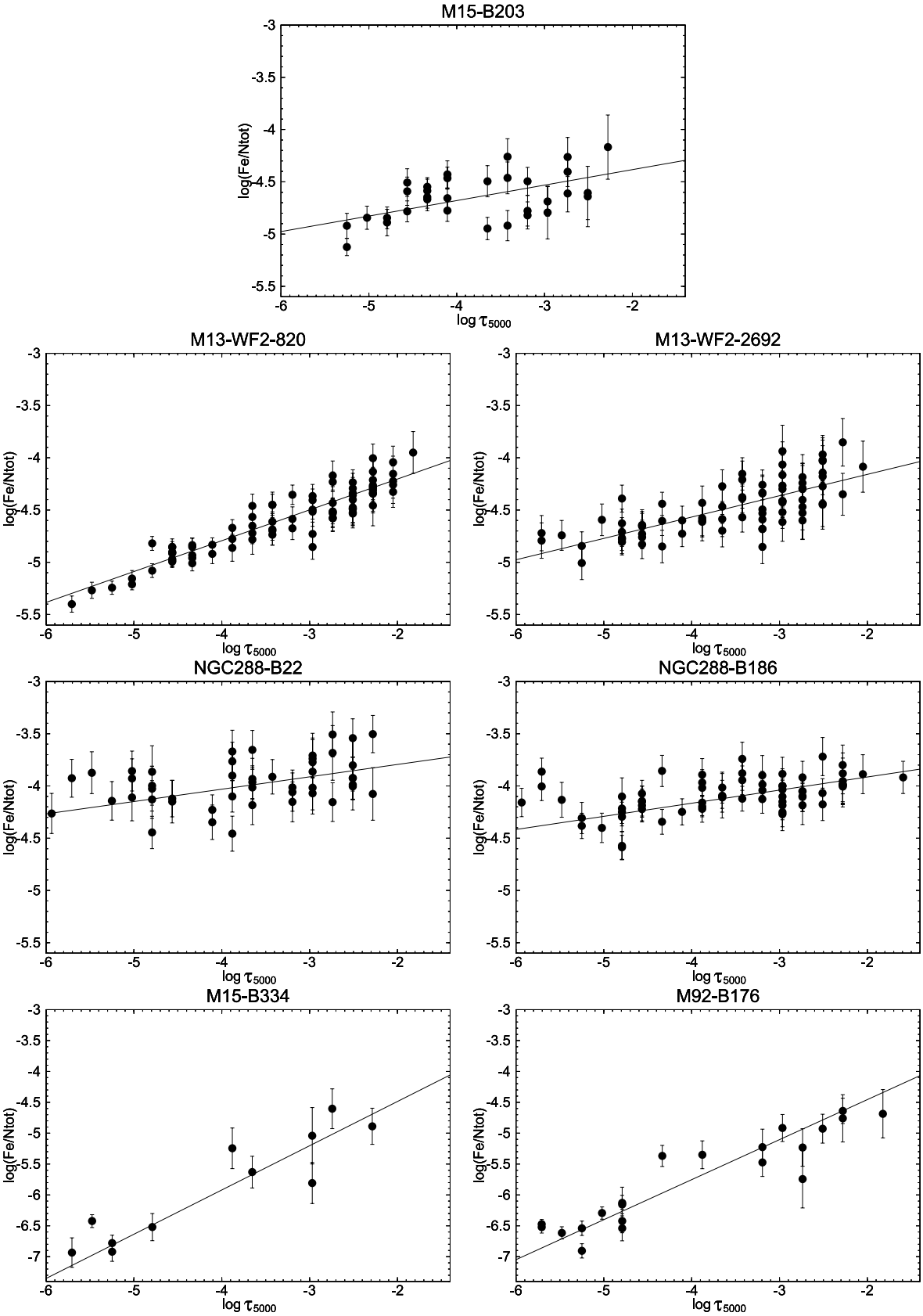

Figure 1. Abundance estimates from the analysis of Fe II (filled circles) lines as a function of line (core) formation optical depth for BHB stars B203 in M15 (middle top), WF 2−820 (second row left) and WF 2−2692 (second row right) in M13, B22 (third row left) and B186 in NGC 288 (third row right), B334 in M15 (bottom left) and B176 in M92 (bottom right). The solid line approximates the data with a linear fit using the least-square algorithm.

Table 3. Data on vertical stratification of iron abundance.

Cluster/star	Fe II		*n*
	Slope	$\log(N_{\rm Fe}/N_{\rm tot})$	
M13/WF 2−820	0.30 ± 0.02	-4.59 ± 0.32	79
M13/WF 2−2692	0.20 ± 0.02	-4.47 ± 0.25	74
M13/WF 2−3123	0.05 ± 0.07	-5.07 ± 0.17	21
M13/WF 3−548	0.04 ± 0.04	-4.99 ± 0.16	26
M13/WF 3−1718	0.02 ± 0.02	-4.36 ± 0.13	96
M15/B203	0.15 ± 0.04	-4.64 ± 0.22	32
M15/B315	0.07 ± 0.03	-4.40 ± 0.21	72
M15/B334	0.72 ± 0.08	-5.89 ± 0.87	11
M15/B374	0.07 ± 0.04	-3.91 ± 0.21	82
M92/B176	0.65 ± 0.07	-5.76 ± 0.75	21
NGC 288/B16	0.01 ± 0.03	-3.81 ± 0.15	42
NGC 288/B22	0.12 ± 0.04	-3.98 ± 0.22	47
NGC 288/B186	0.13 ± 0.02	-4.10 ± 0.17	65
NGC 288/B302	0.06 ± 0.02	-3.73 ± 0.17	75

determination, it is safe to state that iron is vertically stratified in these stars.

4.2 Dependence of stratification on effective temperature

It is clear from the results shown in the previous section and those of Khalack et al. (2007, 2008) that some BHB stars show signatures of vertical stratification of iron abundance, while others do not reveal such a property. All the studied stars (except B334, which has $T_{\rm eff} \simeq 10\,750$ K) have $T_{\rm eff}$ higher than 11 000 K and are therefore in or near the domain of $T_{\rm eff}$ where diffusion is expected to come into play. However, these stars are found in different globular clusters and are shown to have different mean iron abundances. The effective temperature is one of the most important parameter for a stellar atmosphere and has direct impact on the atomic diffusion in BHB stars (Hui-Bon-Hoa et al. 2000; LeBlanc et al. 2009). It would therefore be very interesting to verify if a dependence of vertical iron stratification on $T_{\rm eff}$ exists in BHB stars.

To track possible dependence of iron vertical stratification on $T_{\rm eff}$ we have combined the results obtained in this study with the previously published results by Khalack et al. (2008) for other BHB stars, whose iron abundance slope (see below) was recalculated for the same range of atmospheric depths $-5.3 < \log \tau_{5000} < -2.0$.

The slope of the iron abundance as a function of optical depth for the various BHB stars was calculated and a correlation is found between this slope and $T_{\rm eff}$. Fig. 2 shows the iron slopes with respect to $T_{\rm eff}$, along with a linear fit for these data points using the least-square algorithm (solid line). The stars B334 in M15 and B176 in M92 were excluded from this fit because of the reasons discussed in Section 4.1. They are however shown in Fig. 2 as empty circles. The inclusion of these two stars would not change the qualitative conclusion that the slope of iron abundance decreases as a function of $T_{\rm eff}$ for BHB stars with $T_{\rm eff} \geq 11\,500$ K. The BHB star WF 3−1718 in M13 (shown as empty square in Fig. 2) was also not taken into account during the aforementioned fit depicted by the solid line, because the wings of Balmer lines in its spectrum suggest that a higher $T_{\rm eff}$ is probable for this star. Nevertheless, inclusion of WF 3−1718 still results in some visible correlation (see dashed line in Fig. 2). Adoption of higher effective temperature for WF 3−1718 would amplify this correlation.

The detected correlation indicates that the strongest vertical stratification of iron abundance is expected for BHB stars with $T_{\rm eff}$ near 11 500 K while it decreases for higher values of $T_{\rm eff}$. It becomes negligibly small for the BHB stars with $T_{\rm eff} \geq 14\,000$ K. LeBlanc, Hui-Bon-Hoa & Khalack (2010) find that the theoretical models for BHB stars of LeBlanc et al. (2009) predict a similar tendency of decreasing iron vertical abundance with $T_{\rm eff}$.

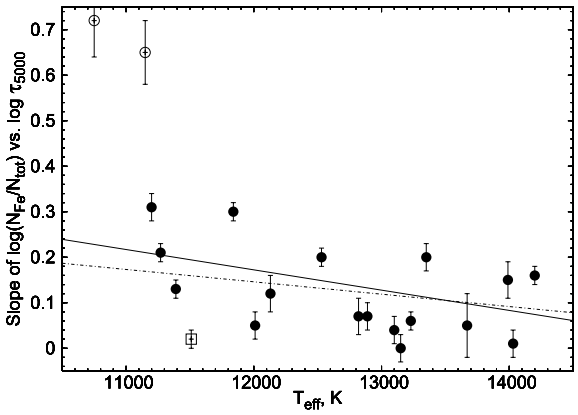

Figure 2. Plot of the slope of iron vertical stratification versus effective temperature of analysed BHB stars (see text for details). The dashed line is a linear fit that includes all stars except for the two stars represented by empty circles (B176 and B334). The linear fit given by the solid line also excludes the star WF 3−1718 represented by the empty square.

5 DISCUSSION

In this paper, we have found additional evidence that iron abundance is vertically stratified in the atmosphere of BHB stars. From the analysis of 14 BHB stars, selected as the most probable candidates for such detections due to their $T_{\rm eff} \geq 11\,500$ K and $V \sin i \leq 10$ km s^{-1}, we have found clear signatures of iron stratification in five stars: B22 and B186 in the globular cluster NGC 288; WF 2−820 and WF 2−2692 in M13 and B203 in M15. Two other stars, B334 in M15 and B176 in M92, show extremely strong increase of iron abundance as a function of optical depth in their atmosphere (see Table 3 and Fig. 2). However, this result may be influenced by the strongly depleted mean iron abundance (that results in a smaller number of analysed line profiles). Furthermore, because of other anomalies found for these two stars (see Section 4.1), some doubts remain about observed stratification of iron in their atmosphere.

For B334 and B176 the effective temperature is only slightly smaller than the limit ($T_{\rm eff} = 11\,500$ K) above which BHB stars show the photometric jumps and gaps (Ferraro et al. 1998; Grundhal et al. 1999) and where diffusion is efficient. On the other hand, Khalack et al. (2008) have shown that stellar atmosphere models with higher $T_{\rm eff}$ usually slightly decrease the slope of the element's abundance with respect to the logarithm of excitation potential as well as with respect to $\log \tau_{5000}$. Therefore, adoption of higher effective temperatures for B334 and B176 will decrease the estimated slopes of iron abundance which increases towards the deeper atmosphere.

The values of effective temperature for the sample of analysed BHB stars were derived from Kurucz's ATLAS9 synthetic photometry grids (Behr 2003a), which use the stellar atmosphere models with homogeneous distribution of element's abundance. Hui-Bon-Hoa et al. (2000) and LeBlanc et al. (2010) have shown that the observable photometric jumps and gaps can be explained in terms of atomic diffusion mechanism that leads to stratification of element's abundance with atmospheric depths. The models with stratified abundance of chemical species result in different

photometric colours as compared to chemically homogenous models. This fact may introduce some errors in the evaluation of $T_{\rm eff}$ by photometric means when using chemically homogeneous atmospheric models. The uncertainty on $T_{\rm eff}$ determination should be studied by using the new atmospheric models of LeBlanc et al. (2009) that take into account vertical stratification of the elements. This is outside the scope of the present paper.

Our analysis of the dependency of the available data for vertical iron stratification in BHB stars with respect to the effective temperature results in the detection of a trend (see Fig. 2). The same results were obtained from the modelling of iron vertical stratification employing the self-consistent stellar atmosphere models with vertically stratified abundance of chemical species (LeBlanc et al. 2010). The results presented here show that for BHB stars with $T_{\rm eff}$ around 11 500 K have the strongest vertical iron stratification gradients. This gradient diminishes as $T_{\rm eff}$ increases up to $T_{\rm eff} \simeq 14\,000$ K, where no significant iron stratification exists. Nevertheless, to statistically improve the registered trend of iron stratification more data for BHB stars with appropriate values of $T_{\rm eff}$ and $V \sin i$, especially for $T_{\rm eff}$ near 11 500 K, need to be analysed. Such additional data will be useful to constrain theoretical model atmospheres that include stratification of elements, similar to those of LeBlanc et al. (2009).

ACKNOWLEDGMENTS

This research was partially funded by the Natural Sciences and Engineering Research Council of Canada (NSERC). We thank the Réseau québécois de calcul de haute performance (RQCHP) for computing resources. BBB thanks all the dedicated people involved in the construction and operation of the Keck telescopes and HIRES spectrograph. He is also grateful to Judy Cohen, Jim McCarthy, George Djorgovski and Pat Côté for their contributions of Keck observing time.

REFERENCES

Behr B. B., 2003a, ApJS, 149, 67
Behr B. B., 2003b, ApJS, 149, 101
Behr B. B., Cohen J. G., McCarthy J. K., Djorgovski S. G., 1999, ApJ, 517, L135
Behr B. B., Djorgovski S. G., Cohen J. G., McCarthy J. K., Côté P., Piotto G., Zoccali M., 2000a, ApJ, 528, 849
Behr B. B., Cohen J. G., McCarthy J. K., 2000b, ApJ, 531, L37
Crocker D. A., Rood R. T., O'Connell R. W., 1988, ApJ, 332, 236
Ferraro F. R., Paltrinieri B., Fusi Pecci F., Dorman B., Rood R. T., 1998, ApJ, 500, 311
Glaspey J. W., Michaud G., Moffat A. F. J., Demers S., 1989, ApJ, 339, 926
Grundahl F., Catelan M., Landsman W. B., Stetson P. B., Andersen M. I., 1999, ApJ, 524, 242
Hauschildt P. H., Baron E., Allard F., 1997, ApJ, 483, 390
Hoyle F., Schwarzschild M., 1955, ApJS, 2, 1
Hubrig S., Castelli F., De Silva G., González J. F., Momany Y., Nepotil M., Moehler S., 2009, A&A, 499, 865
Hui-Bon-Hoa A., LeBlanc F., Hauschildt P. H., 2000, ApJ, 535, L43
Khalack V., Wade G., 2006, A&A, 450, 1157
Khalack V., LeBlanc F., Bohlender D., Wade G., Behr B. B., 2007, A&A, 466, 667
Khalack V., LeBlanc F., Behr B. B., Wade G., Bohlender D., 2008, A&A, 477, 641
Kupka F., Piskunov N. E., Ryabchikova T. A., Stempels H. C., Weiss W. W., 1999, A&AS, 138, 119
Landstreet J. D., 1988, ApJ, 326, 967
LeBlanc F., Monin D., Hui-Bon-Hoa A., Hauschildt P. H., 2009, A&A, 495, 937
LeBlanc F., Hui-Bon-Hoa A., Khalack V. R., 2010, MNRAS, in press
McCarthy J. K., 1990, in Baade D., Grosbøl P. J., eds, Proc. 2nd ESO/ST-ECF Data Analysis Workshop. ESO Conf. and Workshop Proc. Vol. 34. ESO, Garching, p. 119
Michaud G., 1970, ApJ, 160, 641
Moehler S., 2004, in Zverko J., Weiss W. W., Žižňovský J., Adelman S. J., eds, Proc. IAU Symp. 224, The A-Star Puzzle. Cambridge Univ. Press, Cambridge, p. 395
Moehler S., Heber U., DeBoer K. S., 1995, A&A, 294, 65
Moehler S., Sweigart A. V., Landsman W. B., Heber U., Catelan M., 1999, A&A, 346, L1
Peterson R. C., Rood R. T., Crocker D. A., 1995, ApJ, 453, 214
Pickering J. C., Thorne A. P., Perez R., 2001, ApJS, 132, 403
Press W. H., Teukolsky S. A., Vetterling W. T., Flannery B. P., 1992, Numerical Recipes in C: The Art of Scientific Computing, 2nd edn. Cambridge Univ. Press, Cambridge
Quievy D., Charbonneau P., Michaud G., Richer J., 2009, A&A, 500, 1163
Raassen A. J. J., Uylings P. H. M., 1998, A&A, 340, 300
Ryabchikova T. A., Piskunov N. E., Stempels H. C., Kupka F., Weiss W. W., 1999, Phys. Scr. T, 83, 162
Shortridge K., 1993, in Hanisch R. J., Brissenden R. J. V., Barnes J., eds, ASP Conf. Ser. Vol. 52, Astronomical Data Analysis Software and Systems II. Astron. Soc. Pac., San Francisco, p. 219
Thiam M., LeBlanc F., Khalack V., Wade G. A., 2010, MNRAS, 405, 1384
Wade G. A., Bagnulo S., Kochukhov O., Landstreet J. D., Piskunov N., Stift M. J., 2001, A&A, 374, 265

SUPPORTING INFORMATION

Additional Supporting Information may be found in the online version of this article:

Table S1. The full list of analysed spectral lines.

Please note: Wiley-Blackwell are not responsible for the content or functionality of any supporting materials supplied by the authors. Any queries (other than missing material) should be directed to the corresponding author for the article.

This paper has been typeset from a TEX/LATEX file prepared by the author.